

## S5-6-1

# TENSILE CREEP OF UHPFRC UNDER LOW AND HIGH STRESSES

Agnieszka SWITEK

*PhD student, Ecole Polytechnique Fédérale de Lausanne, Switzerland*

Emmanuel DENARIE

*Senior Scientist, Ecole Polytechnique Fédérale de Lausanne, Switzerland*

Eugen BRUEHWILER

*Professor, Ecole Polytechnique Fédérale de Lausanne, Switzerland*

## ABSTRACT

The purpose of this paper is to investigate experimentally the UHPFRC time-dependent behavior under sustained tensile loading and to determine the effect of the stress level on the creep response. Uniaxial tensile creep tests were performed at various stress levels by means of an optimized testing set-up. An Acoustic Emissions equipment was used in parallel to correlate the creep deformations with damage. From 29 % to 85 % stress level, the material exhibited a linear viscoelastic behavior. The UHPFRC response under higher stress levels close to strain hardening remains an open question.

**Keywords:** UHPFRC, tensile creep, strain hardening, stress level, Acoustic Emissions, viscoelasticity

## 1. INTRODUCTION

Ultra High Performance Fiber Reinforced Concretes (UHPFRC) with an extremely dense microstructure and outstanding mechanical properties (compressive strength >150 MPa, tensile strength > 8 MPa, tensile strain hardening), used as local waterproofing and/or reinforcing layers are most adapted for the improvement of the load carrying and protective functions of new or existing structures. The water/binder ratio of UHPFRC is in the range of 0.13 to 0.18, with a dominant autogenous shrinkage. The long term value of the autogenous shrinkage in UHPFRC is not larger than that of usual concretes or SCC. However, in cast-in-situ applications for rehabilitation, as thin layers, under high restraint, it leads to high tensile stresses. These stresses are mitigated by the viscous properties of UHPFRC and at a later stage by their tensile strain hardening response leading eventually to a distributed microcracking at service state. It is thus important to determine the effect of high tensile stresses on the viscous response of UHPFRC, before or within the strain hardening domain. Since many researches have been carried out on the creep properties of cementitious materials in compression, their creep potential in tension is still an open field.

The viscoelastic behavior was barely investigated for UHPFRC material under high tensile stress levels. Kamen [1],[2] investigated UHPFRC creep properties for low and medium stress levels under compression and tension. As expected, specimens loaded at an early age of 3 days showed more basic creep deformation than similar ones loaded at 7 days. At 3 and 7 days, the

stress/strength ratio threshold between linear and non-linear viscoelastic response in compression was around 35%. Kamen et al. [2] showed, on the basis of isothermal tensile tests in a TSTM set-up, that UHPFRC viscous response at early age (3 days) significantly deviates from a linear response when the tensile stress level changes from 32 to 63 %. Further, at very early age (36 to 43 hours) UHPFRC specimens are very sensitive to the age of loading.

Altoubat et al. [3] investigated tensile creep properties of plain and steel fiber reinforced concrete. He showed that the tensile basic creep is very sensitive to the age at loading during the first two days after casting and stabilizes after a few days. Similar tendency was observed by Ostergaard et al. [4] in a study on the basic creep of normal and high-strength concrete. For specimens loaded at very early age of 1 day, the creep response was not proportional to applied stress, which confirms the more pronounced nonlinearity in viscoelastic response for decreasing age of specimen's loading. Bissonnette et al. [5] investigated the tensile creep of plain and steel fiber concrete at 7 days age, for over 60 days. They found that until 50% of the tensile strength, creep deformations were proportional to the applied stress. For High Performance Concrete, Atrushi. [6] showed a threshold of non-linearity for a 60% tensile creep stress level with a loading at 1 day age. At the contrary, Reviron et al [7] observed no significant deviation from a linear viscoelastic response on 6 concrete specimens of 90 days age, tested during 3 days under tensile creep in both sealed and drying conditions, with 50%, 70% and 90% stress levels. Basic creep was surprisingly more than two times smaller than compressive one for a similar concrete, but drying

creep was comparable. According to Bissonnette et al. [8], creep response in compression and in tension for low levels of loading is similar. Similarly, Gutsch et al. [9] found no significant deviation from a linear viscoelastic response of concretes loaded at an age varying from 1 to 28 days under tensile creep or relaxation, at various stress levels, up to 70% of the tensile strength.

On another hand, Al-Kubaisy et al. [10] observed that under tension, above the 70% stress/strength ratio the delayed failure of plain concrete specimens occurred, showing the tendency to non-linear behavior under high sustained load, with time to fracture ranging from few seconds at 95% stress level to 55 h for slightly over 70%. Similar trend was observed by Reinhardt and Cornelissen [11], fracture under sustained loading for concretes occurred with a stress level of 60%, after 5 to 10 days.

From a more fundamental point of view, Acoustic Emission monitoring was used by various authors to qualitatively and quantitatively investigate the onset and development of microcracking during quasi-static or sustained loading tests. Terrien [12], and Saouma et al. [13] among others showed the relationship between fracture processes of concretes in tensile or Wedge Splitting Specimens and AE events (amount and spectrum). The application of AE monitoring to concrete creep testing was done by Rossi et al. [14] to demonstrate the strong correlation between AE events and creep, to outline the dominant role of microcracks development in the basic creep deformations.

The objectives of this paper are to determine the basic creep response of UHPFRC under tension at various stress levels, compare it with existing data, and get insights on the underlying phenomena of the obtained responses by means of AE measurements.

## 2. EXPERIMENTAL

### 2.1. Motivation

Mechanical properties of UHPFRC depend strongly on fiber distribution and orientation in the element. Systematic reproducibility of this material is still a challenge. On another hand, study of basic mechanisms such as tensile creep requires accurate and reproducible testing procedures. For this purpose a comprehensive work was carried out involving optimization of specimen geometry, amount, casting procedure and test equipment and methods to generate representative and reproducible experimental data. Tensile fracture tests were performed with various boundary conditions to determine the fracture response for the investigated material and thus estimate the stress levels in the creep tests.

### 2.2. Materials

The UHPFRC mix used belongs to the CEMTEC<sub>multiscale</sub> family, originally developed by Rossi [15] and tailored for rehabilitation applications at MCS laboratory at EPFL [16]. The ultra compact matrix with a very low water/binder ratio of 0.13 has a high content of paste

(88%) and a high dosage of super plasticizer of 35 kg/m<sup>3</sup> to guarantee a self compacting behavior despite the very high fiber dosage (total 9% vol.). The mixture proportions are given in Table 1.

Table 1 UHPFRC mix composition

Material	Dosage [kg/m <sup>3</sup> ]
Cement	1392
Silica Fume	362
Fine sand (0-0,5mm)	80
Water added	204
Super plasticizer	35
Steel fibers content	706

### 2.3 Specimen preparation

The cross section of the specimens is 70 x 40 mm and their length is 1000 mm. They are cast in formworks placed horizontally on a table to simulate the application of an overlay on a bridge. The room temperature during the mixing was of 16°C and the temperature of the fresh mixes was 20°C. A guiding scoop is used to pour the UHPFRC into the molds following their longitudinal axis to help obtain a reproducible fiber orientation. Two steel rods with bolts at their ends were inserted on both end sides of the specimen for later anchorage in the tensile creep rigs. After pouring, specimens were shortly vibrated by hand and the cure of 20°C and 98 % RH was applied until the loading. Then the not molded surfaces of specimens were surfaced to obtain a uniform thickness. In order to prevent local stress concentrations, 180 mm long aluminum plates are glued on the 70 mm faces of the specimen on both outer sides of the location of the anchorage rods. All specimens were protected from drying until testing and cured at 20°C.

## 3. TENSILE FRACTURE TEST

### 3.1 Testing procedure

Total 8 tensile fracture specimens were tested at 7 days under displacement control with a rate of 0.05 mm/minute, with two different types of supports, fixed and pinned. Four LVDT's with a measurement basis of 600 mm were used, one on each side of the specimen. Two tests series, from two different batches, with pin and fixed supports respectively were performed, as shown on

Fig. 1. With pin supports, rotations are free and cracks are free to propagate asymmetrically from one side of the specimen, leading to a flexural mechanism. At the contrary, with the fixed supports, cracks develop in the symmetric way with respect to the specimen's longitudinal axis. The fixed configuration permits to obtain a material tensile response for a given geometry and the pin configuration permits to better estimate the ultimate stress level applied on creep specimens.

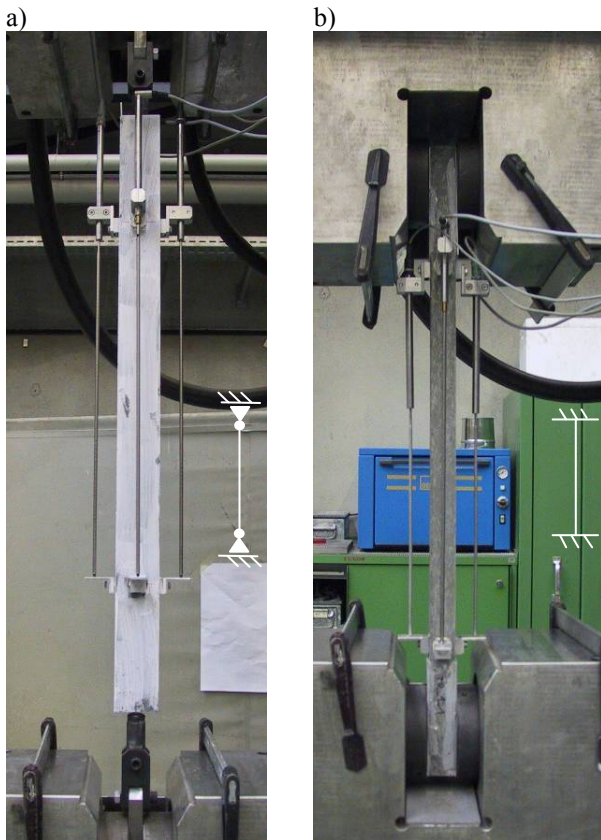


Fig. 1 Tensile fracture test with a) pin supports  
b) fixed supports

### 3.2 Results

Fig. 2 and Fig. 3 present the results of the tensile fracture tests with the fixed (3 specimens) and pin supports (5 specimens). The displacement is the average of the two values given by the two LVDT's set on the 40 mm faces the specimens. The tensile response is described by three domains: 1) nearly linear-elastic part here until on average  $f_{Ut,1st}=9$  MPa, 2) strain hardening with distributed microcracks until the peak at the ultimate tensile strength, here  $f_{Ut,max}=11$  MPa on average and 3) softening, associated to a macro crack opening. Localized fracture occurred in the middle of the specimen, within the measurement basis, which showed that the detail of loading anchorage was not the weakest point. The tensile response obtained in the test with fixed supports is presented on Fig. 2 and with pin supports on Fig. 3. On average, until 0.3 mm displacement, in the strain hardening range, no significant difference can be noticed between the mechanical responses for the two types of boundary conditions. However, as expected, the scatter is larger for the pin supports. The tensile strength estimated from both types of tests is on average 11 MPa and the beginning of the hardening domain is on average 9 MPa.

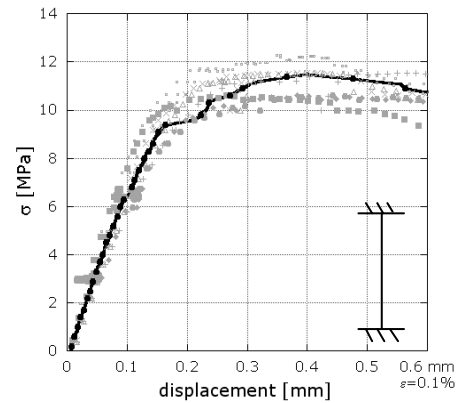


Fig. 2 Average stress-displacement response and measured values, fixed supports

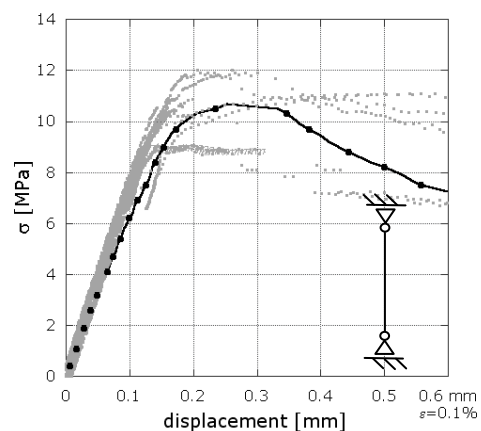


Fig. 3 Average stress-displacement response and measured values, pin supports

## 4. SUSTAINED LOADING TEST

### 4.1 Testing procedure

The time-dependent viscoelastic behavior of UHPFRC was investigated on 15 specimens. For practical reasons, and on the basis of the comparative study presented in § 3., a pin supports system of the creep specimens was selected. The UHPFRC mix was prepared in two subsequent batches to pour 15 specimens: 12 for creep tests and 3 for free shrinkage monitoring. The specimens were wrapped in two layers of Aluminium foil to prevent drying. Three stress levels of 3.2, 6.1 and 9.3 MPa were applied by means of lead weights. From previously presented tensile fracture tests series (see § 3.) performed on a similar material, the first cracking strength  $f_{Ut,1st}$  and ultimate tensile strength  $f_{Ut}$  of the investigated UHPFRC at 7 days were estimated to be respectively on average 9 and 11 MPa. The corresponding stress levels applied in the creep rigs can thus be estimated as 29%, 55% and 85% of  $f_{Ut}$ . This represents low, medium and high stress level respectively. Four specimens were used for each stress level. Load cells were used to monitor the applied load and to determine precisely the starting point of the creep phase, on two specimens out of four for each stress level. Two LVDTs with a measurement basis of



600 mm were installed on each side of the specimens along their 40 mm faces. One AE sensor was attached in the middle of two out of four specimens for each stress level and one on two shrinkage specimens. The AE measurement system used was the SAMOS-8 with 8 sensors connected to two cards incorporated in the instrument. The threshold to record AE waves was of 35 dB and the estimated speed of AE wave propagation in UHPFRC of 2800 m/s. The monitoring was performed during the loading and first days which follow until the stabilization of acoustic emissions activity. Fig. 4 presents the creep specimens in the tensile creep rigs.

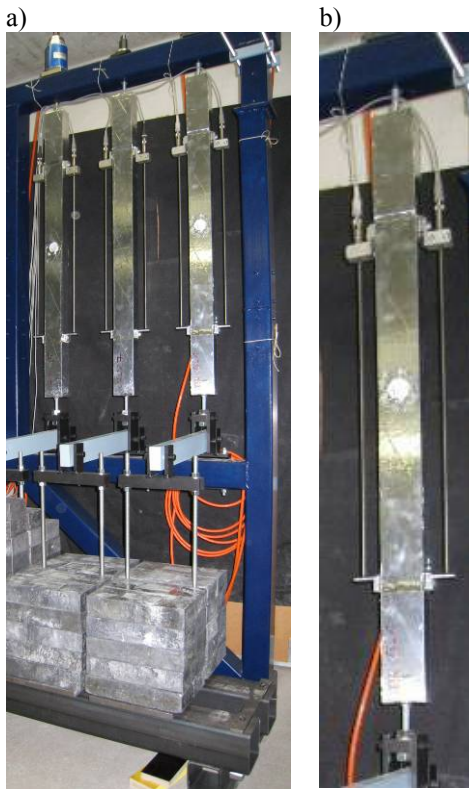


Fig. 4 a) tensile creep test equipment b) tensile creep specimen

#### 4.2. Results and discussion

Shrinkage deformations are presented by points on Fig. 5. Comparison with previously obtained results [1] for a similar material shows good agreement. As expected, Acoustic Emission monitoring didn't show any events. The creep deformation (Fig. 6) was obtained by averaging the displacements measured by each of the two displacement transducers for each specimen. The basic creep deformation for each specimen was obtained by adding the average shrinkage deformation to the average deformation per specimen, measured in the creep rig. Fig. 6 shows the creep deformations of individual specimens and the average curve per each stress level. One can notice the small scatter of the test results.

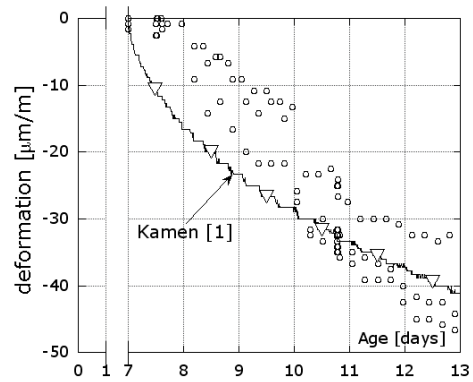


Fig. 5 Free shrinkage of sealed specimens

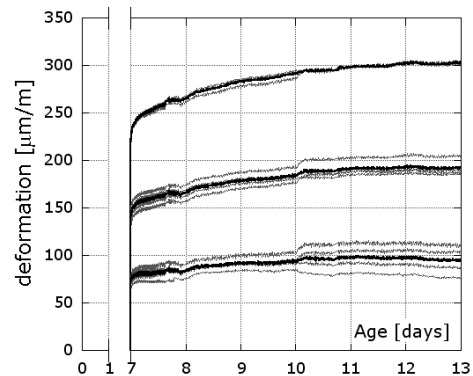


Fig. 6 Basic creep deformation with average curves for the three stress levels

One specimen loaded at the high tensile stress level of 9.3 MPa broke in the few seconds following loading. Since this type of materials can show an important scatter of mechanical properties depending on fiber orientation, this behavior is understandable.

The specific basic creep deformations (elastic plus time-dependent) for three stress levels are presented on Fig. 7. For tensile stress levels of 3.2, 6.1 and 9.3 MPa, representing 29%, 55% and 85% of  $f_{U,t}$  respectively, the instantaneous elastic deformation is proportional to the applied stress level within the scatter range. The average specific basic creep deformation (Fig. 7) deviates slightly from linearity for high level, showing about 1 [ $\mu\text{m/m/MPa}$ ] of difference from lower stress levels. This difference is however within the scatter range of the measurement for all stress levels, illustrated on Fig. 6. Comparatively, Atrushi [6], states deviation from linearity for concrete specimens, above 70% stress/strength level for 10 [ $\mu\text{m/m/MPa}$ ] of difference in comparison with lower levels. On that basis the very slight deviation from linearity observed on average curves for 9 MPa stress level is too small to be interpreted as a non-linear viscoelastic response. Experiments with higher stress levels above 85% of  $f_{U,t}$  are needed to bring to light non-linear behavior of UHPFRC.

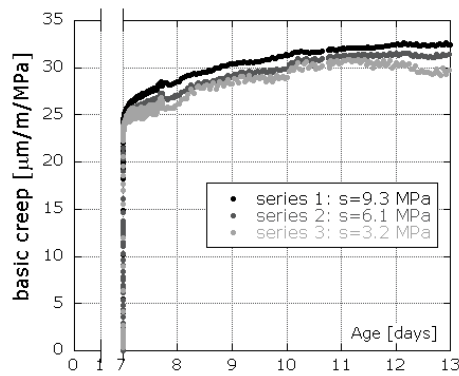


Fig. 7 Average specific basic creep for the three stress levels

At the contrary, for a closely related material, but loaded earlier at 3 days, the dependence of specific basic creep deformation on stress/strength ratio was observed [2], showing the onset of non-linear viscoelastic response above 35% of  $f_{U,t}$ , and tertiary creep indices above 65% of  $f_{U,t}$ . From a general point of view, it appears that the maturity at loading (and also the degree of hydration), plays a dominant role on the threshold value for the onset of non-linear viscoelasticity [1], [2], [5], [6], [9].

#### 4.3 Acoustic Emissions monitoring

Acoustic emission event corresponds to the release of the elastic energy due to damage propagation during deformation evolution. For the investigated UHPFRC with steel fibers, it is most likely to correspond to micro- and macro-cracking of the cementitious matrix and in the softening part, after the macro-crack opening, to the fibers pull-out. Since the stress level applied on the specimens is inferior to the estimated first cracking strength, the recorded events are associated to micro cracking of the matrix. Acoustic Emissions monitoring results are presented for the first 7 hours after loading. On Fig. 8 we can notice a strong correlation between the Acoustic Emission cumulative hits curve and the creep deformation for 9.3 MPa stress level. A similar trend was observed for 6.1 and 3.2 MPa stress levels.

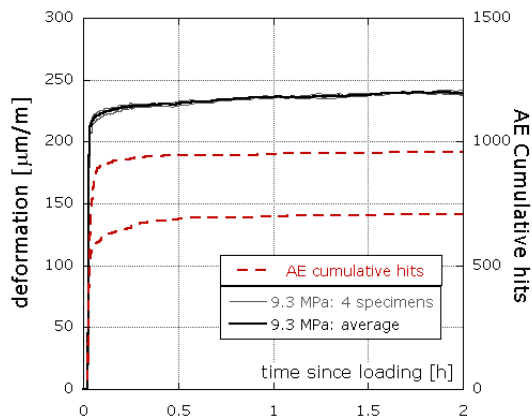


Fig. 8 Deformation and AE events for 9.3 MPa stress level

The cumulative number of hits only is not sufficient information to characterize the creep deformation process. Additional information on amplitude and energy of the events for 9.3 MPa stress level is presented on Fig. 9. The amplitudes of the events recorded during the deformation show two domains of activity. First domain is when the AE events are continuous and their number increases during loading. Second one during the sustained loading phase shows less activity, where AE events and deformations rates stabilize. For all stress levels, the amplitude of the AE events was of the same magnitude, inferior to 65 dB, likely to be associated to a similar origin, interpreted as microcracking.

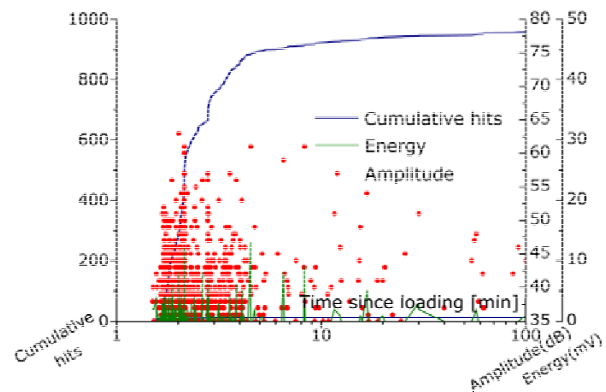


Fig. 9 Total number of hits, energy and amplitude for one 9.3 MPa stress level specimen

Fig. 10 shows the cumulative number of hits for all monitored specimens, (2 per stress level). After 7 hours from the loading time we can observe a higher number of AE events for 9.3 MPa stress level between 700 and 1000 and lower AE events number of 70-180 and less than 30 for 6.1 and 3.2 MPa stress levels respectively. The reason for the difference between the results for two specimens for each stress level is still unclear but might be due to the variability of the fibrous mix of the material, although no such differences can be observed on the measured deformations (Fig. 7). Further, for the high stress level fracture occurred in one of the specimens just after loading.

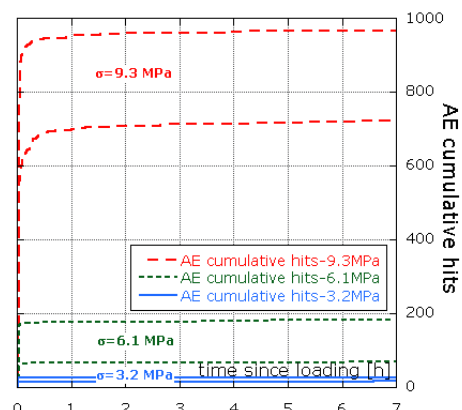


Fig. 10 Total number of AE hits for each stress level

## 5. CONCLUSIONS

- (1) A tensile creep set-up was developed to accurately determine the tensile creep response of UHPFRC. The small scatter of test results showed the efficiency of the set-up.
- (2) Basic tensile creep tests at 7 days age on a UHPFRC, with 3.2, 6.1 and 9.3 MPa, estimated as 29%, 55% and 85% of  $f_{U,t}$  respectively, showed a linear viscoelastic response for all stress levels.
- (3) Strong correlation between strains and AE number of events in time confirms that Acoustic Emission monitoring is a good supplementary technique to qualitatively analyze the concrete creep deformations.
- (4) The same level of amplitude and energy released during the loading and sustained load shows that micro cracks are at origin of tensile creep deformation.

## ACKNOWLEDGEMENT

This project was financially supported by the European community through the 6<sup>th</sup> FP project ARCHES and by the Swiss National Science Foundation. The authors would like to express their sincere thanks to MM. Hadi Kamyab and Alain Proust for their major contribution to Acoustic Emissions measurements and Roland Gysler for his precious technical support on experimental setups.

## REFERENCES

1. Kamen A., "Comportement au jeune âge et différé d'un BFUP écouissant sous les effets thermomécaniques" PhD thesis N°3827, EPFL, June 2007.
2. Kamen A., Denarié E., Sadouki H., Brühwiler E., "UHPFRC tensile creep at early age" Materials and Structures, N°42, 2008, pp.113-122.
3. Altoubat S.A., Lange D.A., "Tensile basic creep: measurements and behaviour at early age" ACI Materials Journal, September-October 2001, pp.386-393.
4. Ostergaard L., Lange D.A., Altoubat A.S., Stang H., "Tensile basic creep of early-age concrete under constant load" Cement and Concrete Research, N°31, 2001, pp.1895-1899.
5. Bissonnette B., Pigeon M., Vaysburd A.M., "Tensile creep of concrete: study of its sensitivity to basic parameters" ACI Materials Journal, July-August 2007, pp.360-368.
6. Atrushi D.S., "Tensile and compressive creep of early age concrete: testing and modelling" PhD thesis N°3377, Norwegian University of Science and Technology, Trondheim, Norway, March 2003.
7. Reviron N., Nahas G., Tailhan J.-L., Le Maou F., "Experimental study of uniaxial tensile creep of concrete" Concreep 8 Conference Proceedings, 2009, pp.453-457.
8. Bissonnette B., Boily D., Bastien J., Fafard M., "Tensile creep of concrete repair materials: recent experimental findings towards optimization" Concreep 6 Conference Proceedings, August 2001, pp.599-604.
9. Gutsch A., Rostásy F.S., "Young concrete under high tensile stresses-creep relaxation and cracking" R. Springenschmidt (Ed.), Proceedings RILEM Symposium 'Thermal Cracking in Concrete at Early Ages', Chapman & Hall, London, 1995, pp.111-116.
10. Al-Kubaisy M.A., Young A.G., "Failure of concrete under sustained tension", Magazine of Concrete Research: Vol. 27, N°92, September 1975, pp.171-178.
11. Reinhardt H.W., Cornelissen H.A.W., "Zeitstandzugversuche an Beton", Baustoffe 85, Bauverlag, Wiesbaden, 1985, pp. 162-167.
12. Terrien M., "Emission Acoustique et comportement mécanique post-critique d'un béton sollicité en traction", Bulletin de Liaison Labo. Ponts et Chaussées N°105, 1980, pp. 65-72.
13. Saouma V. E., Broz J. J., Brühwiler E., Boggs H. L., "Effect of aggregate and specimen size on fracture properties of dam concrete", J. of Materials in Civil Engineering, Vol. 3, No. 3, August, 1991, pp. 204-218.
14. Rossi P., Godart N., Robert J. L., Gervais J. P., Bruhat D., "Investigation of the basic creep of concrete by acoustic emission", Materials and Structures, Vol. 27, 1994, pp. 510-514.
15. Rossi P., "Development of new cement composite material for construction", Innovations and Developments in Concrete materials and Construction, Proceedings of the International Conference, University of Dundee, Scotland, September 2002, pp.17-29.
16. Wuest J., "Comportement structural des bétons de fibrés ultra performants en traction dans des éléments composés", PhD thesis N°3987, December 2007.